On the Role of Stiffness and Synchronization in Human-Robot Handshaking

Domenico Mura[1], Espen Knoop[2], Manuel G. Catalano[3], Giorgio Grioli[3], Moritz Bächer[2], Antonio Bicchi[1,3]

Abstract

This paper presents a system for soft human-robot handshaking, using a soft robot hand in conjunction with a lightweight and impedance-controlled robot arm. Using this system, we study how different factors influence the perceived naturalness, and give the robot different personality traits. Capitalizing on recent findings regarding handshake grasp force regulation, and on studies of the impedance control of the human arm, we investigate the role of arm stiffness as well as the kinaesthetic synchronization of human and robot arm motions during the handshake.

The system is implemented using a lightweight anthropomorphic arm, with a Pisa/IIT Softhand wearing a sensorized silicone glove as the end-effector. The robotic arm is impedance-controlled, and its stiffness changes according to different laws under investigation. An internal observer is employed to synchronize the human and robot arm motions. Thus, we simulate both active and passive behaviour of the robotic arm during the interaction.

Using the system, studies are conducted where 20 participants are asked to interact with the robot, and then rate the perceived quality of the interaction using Likert scales. Our results show that the control of the robotic arm kinaesthetic behaviour does have effect in the interaction with the robot, in term of its perceived personality traits, responsiveness and human-likeness. Our results pave the way towards robotic systems that are capable of performing human-robot interactions in a more human-like manner, and with personality.

1 INTRODUCTION

Humans are soft, and inherently exploit softness when interacting with their environment and with each other. This softness appears in the muscles and tendons, which are naturally elastic and backdrivable, as well as in the skin, where the subcutaneous tissue causes fingers to conform to objects that are being grasped. As we progress towards robotic systems which are capable of convincing and human-like interactions with the environment and with humans, it will become increasingly important for these systems to exploit softness in this same way, particularly if they are designed for physical Human-Robot Interaction (pHRI).

Handshaking (Fig. 1) is an interesting interaction to study in this regard: while seemingly simple, handshakes combine cutaneous elements, of hand-hand contact, with kinaesthetic elements, of the consensus arm motion. Handshakes are common greeting interactions throughout the world (Dolcos et al. 2012), and have strong social connotations, which means that humans have a clear prior expectation of what a handshake should feel like.

Human-robot handshaking has received some attention in the literature, but, to date, the majority of studies focused on specific aspects of the interaction.

The kinaesthetic aspect of handshaking has been studied by Giannopoulos et al. (2011), where a haptic device with a metal rod as an end effector was used to simulate handshakes in order to enhance the physicality of an immersive virtual environment. The same authors also investigated the use

Figure 1. The human/robot handshake between an anthropomorphic impedance controlled manipulator, equipped with a sensorized Pisa/IIT SoftHand, and a human.

of Hidden Markov Models to estimate consensus motions

[1] Centro di Ricerca "E. Piaggio", Univ. di Pisa, Pisa, Italy
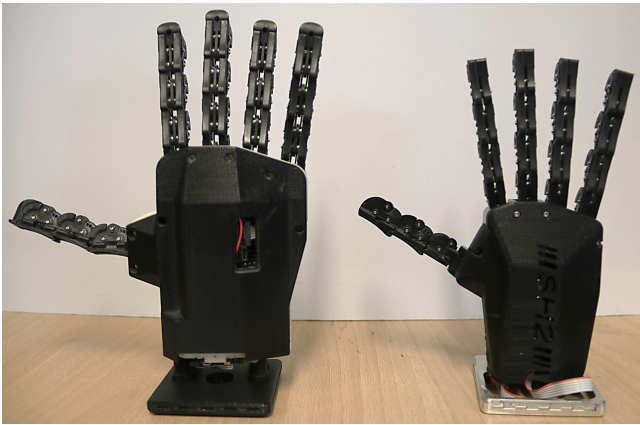[2] Disney Research, Zurich, Switzerland
[3] Dept. of Soft Robotics for Human Cooperation and Rehabilitation, Istituto Italiano di Tecnologia, Genoa, Italy.
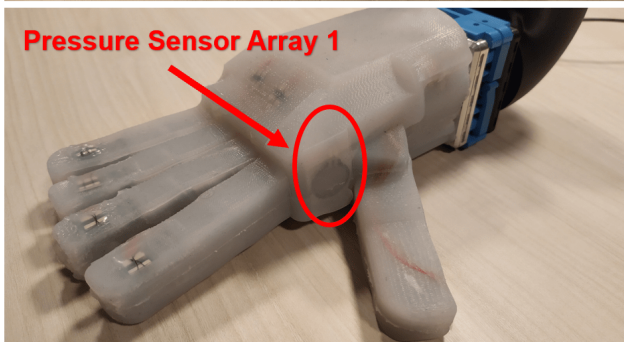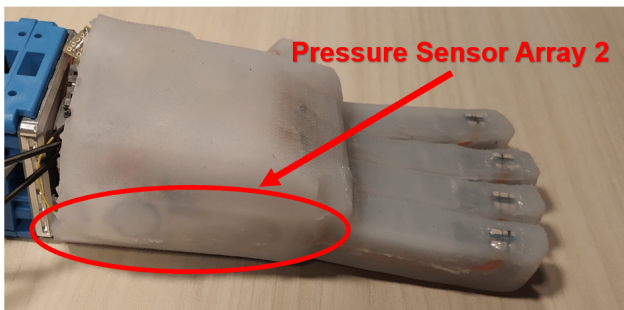
Corresponding author:
Domenico Mura, Centro di Ricerca "E. Piaggio", Univ. di Pisa, Pisa, Italy.
Email: domenico.mura@phd.unipi.it

(a)

(b)

Pressure Sensor Array 2

Pressure Sensor Array 1

(c)

Figure 2. a) The experimental setup with both the anthropomorphic arm and the gloved SoftHand. b) The original SoftHand version (on the left) confronted with the more compact version (on the right) we employed in the setup to enhance the handshake ergonomics. c) The custom-made silicon glove used in this study, with its embedded sensorization highlighted.

(Wang et al. 2009). Moreover, Avraham et al. (2012) and Papageorgiou and Doulgeri (2015) present examples of different motion models for consensus handshaking. Related to this line of research, Jindai et al. (2015) focus on a robot simulating also the approaching motions before the handshake, i.e. before the hands make contact.

Another important aspect to understand in this regard is the arm impedance. It is known that human arm stiffness is modulated depending on the task (Ajoudani et al. 2012). Some works have studied how to mimic the impedance regulation of humans in robotic systems, e.g. Bhattacharjee and Niemeyer (2015), but to date this has not been considered in the context of handshake tasks.

Conversely, works focusing on the cutaneous elements of the interactions include Orefice et al. (2018) and Knoop et al. (2017), where the feasibility of soft robotic hand use is also exploited. Vigni et al. (2019) highlight the importance of analysing interaction forces between human and robot hand, and study the use of closed-loop feedback hand control.

While such targeted studies are informative stepping stones, it is only with a complete interactive system that one can begin to study how the interaction as a whole is perceived, and move towards robotic systems capable of conveying expressions and emotions through their behaviour. There exist only a few recent examples of complete systems for handshaking, e.g. by Tsalamlal et al. (2015), where the relative importance of haptic and visual cues is studied. Recently, Arns et al. (2017) presented a fast and reactive system for human-robot handshaking, adopting a custom robot hand. Avelino et al. (2018b) also implement a handshaking system on an anthropomorphic robot, and investigate the effect of handshake gripping strength. However, in these applications the robot is either passive w.r.t. the interaction, or it employs control laws which are insensitive to the subject unique and simultaneous kinaesthetic/haptic features.

In this study, we investigate different handshake strategies, aiming to relate the robotic arm stiffness, its synchronization with the human, and their overlapping role during the handshake. To this end, we develop a complete system for handshaking that combines a soft hand, an impedance-controlled arm and a sensorized silicon glove, shown in Fig. 2. It exploits both kinaesthetic softness, through an impedance-controlled arm and an underactuated hand, and cutaneous softness, through a soft silicone glove. This is implemented on a FRANKA robot arm, and uses a Pisa/IIT SoftHand with a custom-made silicone glove, which is sensorized to allow the detection of human grasping force similarly to Vigni et al. (2019). The system incorporates an Extended Kalman Filter (EKF) in order to learn the parameters of a human shaking motion and mimic it, for a consensus behaviour. The hand is controlled in a closed-loop manner depending on the applied force.

We implement 3 different controls with varying impedance behaviour and 2 controls for the arm motion, then we combine them for a total of 6 control strategies on the arm behaviour. Using our system, we conduct a user study where participants are first asked to interact with the different controllers and rate them using Likert scales in terms of i) quality of the handshake, ii) human-likeness of the handshake, iii) responsiveness of the robot, iv) the

Strategy	Stiffness	Synchronization
C_1	K_{MAX}	Active
C_2	K_{MAX}	Inactive
C_3	K_{MIN}	Active
C_4	K_{MIN}	Inactive
C_5	K_{VAR}	Active
C_6	K_{VAR}	Inactive

Table 1. Implemented Control Strategies for the Robotic Arm Behaviour

perceived leader of the interaction, and v) the perceived personality (introvert/extrovert) of the robot. In a second part of the experiment, subjects are asked to rank the controllers in a forced-choice manner. Our preliminary results of the first part of the experiment show that the different controllers exhibit variations in the perceived personality of the robot, on its human-likeness and its responsiveness. From these results, we posit that the developed system is well suited for investigating human perception of robot behaviours, and that it could also play a role in defining how robots can mimic/exhibit social interaction skills in order to communicate emotions to people.

2 EXPERIMENT DESIGN

In this paper, we implement different handshake strategies, controlling and modulating the robotic arm stiffness and its active/synchronized behaviour during the handshake.

The synchronization of the human/robot handshake motion is obtained by an internal observer that generates a cartesian pose reference for the robot. The robotic arm can switch between 2 modes of operation: i) passive motion, provided by the impedance control; and ii) active, synchronized motion related to the kinaesthetic features of the human handshaking motion. A detailed discussion of the reconstruction of the human reference motions is provided in Secs. 3.3, 3.4 and 3.5.

To exploit the effect of the arm stiffness modulation on the whole interaction, we implement 3 different control strategies for the stiffness of the robot impedance control, setting it to: i) a constant high stiffness K_{MAX}; ii) a constant low stiffness K_{MIN}; and iii) a variable stiffness K_{VAR}, related to the handshake grasp force exerted by the human on the robotic hand. We develop this set of controllers with varying impedance behaviour to investigate the quantitative relation between the human arm adaptable stiffness and the handshake interaction, which has thus far received little study. More details on the robotic arm stiffness modulation are provided in Sec. 3.6.

In summary, we define and use here 6 control strategies for the arm behaviour, which arise from the intersection between 3 stiffness control laws (constant high stiffness K_{MAX}, constant low stiffness K_{MIN}, variable stiffness K_{VAR}) and 2 different kinaesthetic control laws (synchronization enabled $\rightarrow$ active mode, synchronization disabled $\rightarrow$ passive mode). The arm strategies, labelled from C_1 to C_6, are listed in Table 1. For all the experiments, we use the same hand closure control strategy.

3 MATERIALS AND METHODS

3.1 Robotic Arm and Hand

Here, and in the following section, we present the hardware setup used to obtain the results presented in this work.

The robotic arm used in this paper is a lightweight 7-DoF FRANKA Emika manipulator*. It is controlled in a *ROS*-based framework with impedance control. Thus, the robot reacts as a mass-spring-damper system to the human stimuli at its end-effector, where the spring stiffness (i.e. the impedance control cartesian stiffness matrix) is set with a dedicated *ROS* node in order to execute the stiffness control strategies.

A right Pisa/IIT SoftHand (Catalano et al. 2014) is used as the robot end-effector, to be grasped and shaken by the human hand. The adaptability of the hand joints to various types of grasps make it well suited for this scenario, and it has also previously been used in handshakes studies (Vigni et al. 2019). We note that in this work, we used a version of the SoftHand with a reduced and more compact factor form (especially regarding the palm) w.r.t. the original one, in order to enhance the handshake ergonomics. Fig. 2b shows the difference in factor form between the first version of the SoftHand (left) and the version employed in this work (right). The hand is controlled by another *ROS* node connected to the general framework.

3.2 Sensorized Glove

As the Pisa/IIT SoftHand is not sensorized in itself (Catalano et al. 2014), we designed a custom-made silicon glove in order to detect the handshake contact forces with a human hand, to be used in the control laws of the hand. Our glove, shown in Fig. 2c, capitalizes on recent studies on human-robot handshaking (Knoop et al. 2017; Vigni et al. 2019). Its functionality is twofold: on the one hand, it integrates the sensor in its silicone matrix and, as a consequence, i) it is a non-invasive add-on to the device, and ii) it provides mechanical protection for the sensors. On the other hand, the glove provides cutaneous softness, which is beneficial from the point of view of the handshake quality.

The cutaneous softness addresses an issue raised in Knoop et al. (2017), where it was found that the hard plastic fingers of the SoftHand lead to localized pressure peaks in the handshaking grasp, which can cause discomfort even at low grasping forces. This result was a further motivation for us to employ a soft silicone glove.

To detect the human-robot handshake forces, two FSR (Force Sensitive Resistor) pressure sensor arrays are placed inside channels molded into the glove, at expected hand contact locations as found by Knoop et al. (2017). Specifically, two sensors are placed on the glove back, corresponding to the hand metacarpal zone, near the thumb articulation. Three further sensors are placed on the lateral surface of the glove, corresponding to the lateral side of the ulnar palm zone. The placement of the FSR sensors on the robotic hand is shown in Fig. 3b. It can be seen from Fig. 3a that the sensors match the 100% handshake contact zones
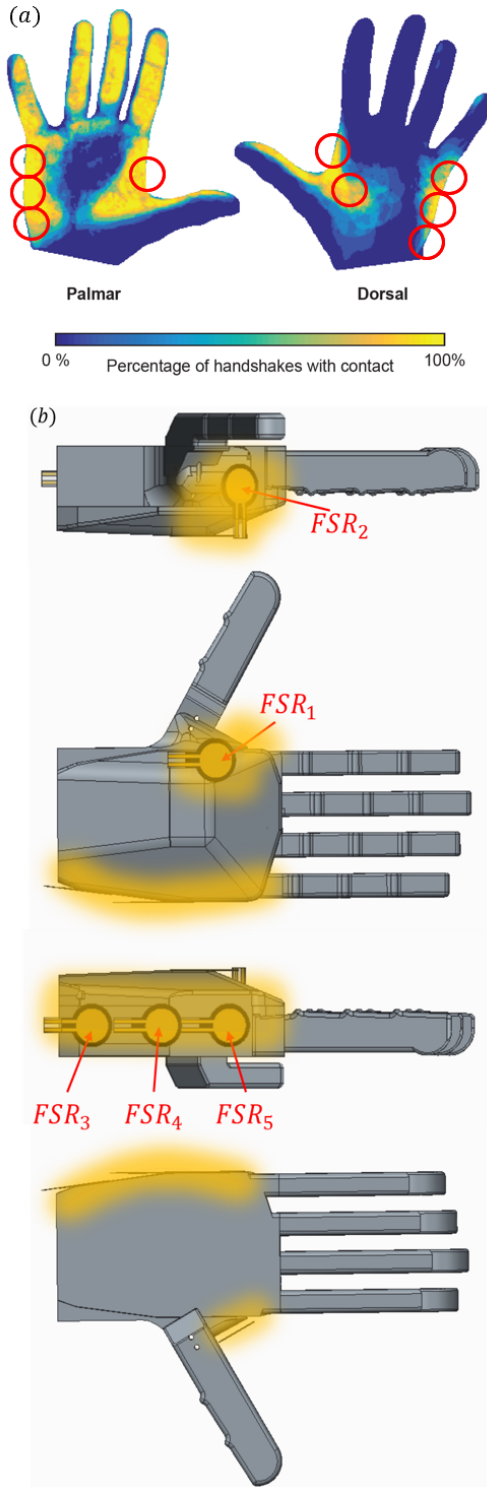
---

*https://www.franka.de/

Figure 3. a) Placement of the FSR sensors, indicated in red circles, w.r.t. the 100% handshake contact zones for the hand dorsal part identified in Knoop et al. (2017). b) Placement of the FSR sensors in the robotic hand (a simplified CAD with the form factor of the SoftHand is shown). The influence areas of the sensor on the hand metacarpal zone and on the lateral side of the ulnar palm zone are highlighted with a yellow glow, to be compared with a).

for the hand dorsal part identified in Knoop et al. (2017). No sensors are placed on the fingers or the palm.

A chamber on the glove dorsal zone houses an electronic board, which records and processes the readings from the

FSR sensors, along with a custom analog RC circuit which performs a first low-pass filtering of the pressure sensor data. More details about the electronics and control of the system are provided in Della Santina et al. (2017).

The glove fabrication is further described in Appendix A.

3.3 Human-Robot Interaction Modelling

Two (robotic or human) arms performing a handshake can be modelled as a constrained dynamic problem, where two serial manipulators are joined by a compliant constraint at their end-effectors (i.e. hands). Let us assume that we have no information about one of the manipulators, which represents the human side of the interaction (i.e. no sensor is to be placed on the human). In this case, its arm dynamics can be neglected and reduced to an external torque applied at the robotic manipulator end-effector. The robot dynamic system can be modelled as

$$\mathbf{B}(\mathbf{q})\ddot{\mathbf{q}} + \mathbf{C}(\mathbf{q},\dot{\mathbf{q}})\dot{\mathbf{q}} + \mathbf{G}(\mathbf{q}) = \boldsymbol{\tau}_m - \mathbf{J}^T(\mathbf{q})\mathbf{h}_{ext}, \quad (1)$$

where $\mathbf{B}$, $\mathbf{C}$ and $\mathbf{G}$ are, respectively, the inertia, Coriolis and gravity matrices of the manipulator, $\mathbf{J}$ is the Jacobian matrix, and $\mathbf{q}$ and $\boldsymbol{\tau}_m$ are the vectors of joint coordinates and torques. We assume that the constraint between the two arms, i.e. the interaction wrench at the end-effector $\mathbf{h}_{ext}$, is generated by a viscoelastic model so that $\mathbf{h}_{ext} = \mathbf{K}(\mathbf{p}_{ee} - \mathbf{p}_h) + \mathbf{F}(\boldsymbol{\xi}_{ee} - \boldsymbol{\xi}_h)$, where $\mathbf{p}_{ee}$ and $\mathbf{p}_h$ are the poses of the robotic end-effector and of the hand, $\boldsymbol{\xi}_{ee}$ and $\boldsymbol{\xi}_h$ are the corresponding velocities, and $\mathbf{K}$ and $\mathbf{F}$ are two positive-definite and symmetrical matrices which take into account, respectively, the elastic and damping action of the constraint (Siciliano et al. 2010).

For our case, we can simplify the model by restricting the dynamical system of (1) to a 1 DoF case, where the handshake motion occurs only along the vertical direction, as already done in previous studies on handshake kinaesthetics (Papageorgiou and Doulgeri 2015). Moreover, we can model the entire robotic manipulator as a mass-spring-damper system through the use of impedance control. Thus, (1) simplifies to a second order system as

$$\begin{cases} \dot{q}_1 = q_2; \\ m_R\dot{q}_2 = C_H(q_2 - \dot{z}_H) + K_H(q_1 - z_H) + \\ \quad + C_R(q_2 - \dot{z}_R) + K_R(q_1 - z_R), \end{cases} \quad (2)$$

where the manipulator has a total mass m_R, concentrated at its end-effector, and C_R and K_R are, respectively, its stiffness and viscous damping coefficients. The mass m_R is also connected to a spring and a damper with elastic and viscous damping coefficients K_H and C_H, representing the compliant handshake coupling. Thus, it can be seen that $q_1 = z_{EE}$ and $q_2 = \dot{z}_{EE}$ are the position and velocity of the robot end-effector. They depend on both i) z_H and $\dot{z}_H$, the position and velocity of the handshake transmitted by the human to the end-effector, and on ii) z_R and $\dot{z}_R$, the same quantities relative to the end-effector motion imparted by the manipulator impedance control. This simplified model is shown in Fig. 4. The numerical values of K_R, K_H, C_R and C_H are chosen in accordance with the literature on human arm cartesian impedance (Dolan et al. 1993; Artemiadis et al. 2010; Tsuji et al. 1995).
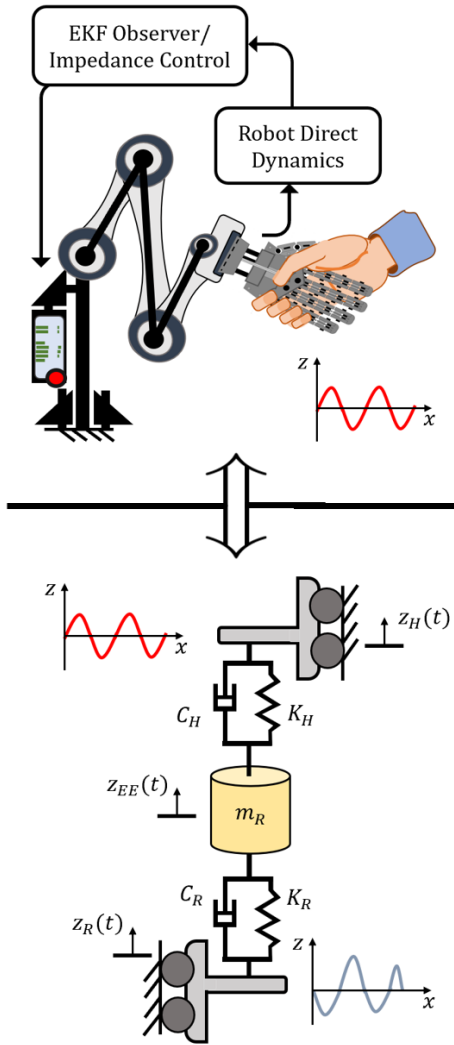
Figure 4. Human-robot handshake, modelled as a mass-spring-damper system connected with a compliant constraint to an external object which exhibits a sinusoidal motion. The numerical values of K_R, K_H, C_R and C_H are chosen in accordance with the literature on the human arm cartesian impedance.

3.4 Reconstruction of the Human Reference Motions

When trying to assess the state of the handshake, referring to (2), z_R and $\dot{z}_R$ can be reconstructed from the readings of the robot joints through direct kinematics, but z_H and $\dot{z}_H$ cannot be measured. We employed an Extended Kalman Filter (EKF) to observe the system, as it is desirable to have a human-robot handshaking framework that does not require the human to wear additional sensors or instrumentation. Moreover, we require that in order to simulate an active behaviour for a handshake, the robot should synchronize to the human partner.

To obtain this goal, i.e. i) synchronize to the human signature motion and ii) simulate an active/leading behaviour by anticipating it, we designed the EKF to observe the intention of the human, and to command an appropriate control reference for the arm. We describe here the state-space modelling of the system to be observed by the EKF, while we describe the definition of the control reference

for human-robot synchronization in Sec. 3.5. As the system cannot measure the intention of the human side, it is assumed here to be a sinusoidal wave of unknown time-varying amplitude and frequency. Thus, the handshake motion terms z_H and $\dot{z}_H$ arise from a sinusoidal function with variable amplitude $A(t)$ and offset $O(t)$, namely $h(t)$, i.e.

$$h(t) = A(t)\sin(\omega t + \phi) + O(t). \tag{3}$$

This function is obtained by the dynamics of a single DoF harmonic oscillator along the vertical direction, i.e. $\ddot{z}_H = -\omega^2 z_H$, which is modelled in state-space as

$$\begin{cases} \dot{\alpha}_1 = \alpha_2\alpha_4; & \alpha_1 = z_H; \\ \dot{\alpha}_2 = -\alpha_1\alpha_4; & \alpha_2 = \dot{z}_H/\omega; \\ \dot{\alpha}_3 = 0; & \text{where:} & \alpha_3 = O; \\ \dot{\alpha}_4 = 0; & \alpha_4 = \omega. \end{cases} \tag{4}$$

As seen from (4), α_3 and α_4 are constant states representing the sinusoidal offset and frequency, respectively. They are adjoined to the system so to be estimated via the output equation

$$y(t) = \alpha_1 + \alpha_3 = z(t) + O(t). \tag{5}$$

Considering that $z(t) = A(t)\sin(\omega t + \phi)$, from (5) one can resolve the expression of $h(t)$. Moreover, the sinusoid amplitude can be estimated from $A(t) = \sqrt{\alpha_1^2 + \alpha_2^2}$. Bringing together (4) and (2), the entire system becomes a constrained dynamic problem, where the mass m_R is connected to a slider with a sinusoidal motion through the handshake compliant coupling. Its complete state vector is defined as $\mathbf{x} = [\,\boldsymbol{\alpha}\,|\,\mathbf{q}\,]^T$, where $\boldsymbol{\alpha} = [\,\alpha_1\,,\,\alpha_2\,,\,\alpha_3\,,\,\alpha_4\,]^T$ are the handshake motion constraint states and $\mathbf{q} = [\,q_1\,,q_2\,]^T$ represents the physical system states.

A preliminary observability analysis on the system verified the feasibility of the estimation process from only end-effector position measurements. The same analysis proved the filter low parametric sensitivity, i.e. its robustness to inaccurate physical parameters in the EKF prediction part. The system model is discretized with a Forward Euler approach. Thus, setting a time step equal to Δt, the complete dynamics at time k become

$$\begin{cases} \alpha_{1,k+1} = \alpha_{1,k} + \Delta t\alpha_{2,k}\alpha_{4,k}; \\ \alpha_{2,k+1} = \alpha_{2,k} - \Delta t\alpha_{1,k}\alpha_{4,k}; \\ \alpha_{3,k+1} = \alpha_{3,k}; \\ \alpha_{4,k+1} = \alpha_{4,k}; \\ q_{1,k+1} = q_{1,k} + \Delta t q_{2,k}; \\ q_{2,k+1} = q_{2,k} + [C_H(q_{2,k} - \dot{z}_{H,k}) + K_H(q_{1,k} - z_{H,k}) + \\ \quad + C_R(q_{2,k} - \dot{z}_{R,k}) + K_R(q_{1,k} - z_{R,k})]/m_R. \end{cases} \tag{6}$$

After the update of the state vector, $\mathbf{x}_{k+1}$ is used to evaluate online the state Jacobian of the EKF.

3.5 Human-Robot Synchronization

After convergence, from the status of the EKF it is possible to reconstruct the features of the sinusoidal wave that represents the handshaking motion exerted by the human on the robot end-effector. The terms z_H and $\dot{z}_H$ in the expression for $q_{2,k+1}$ in (6) are computed as
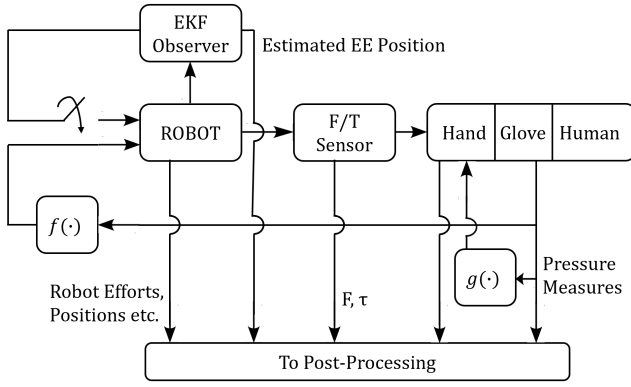
Figure 5. Scheme of the implemented control/estimation architecture. The pressure measurements that carry the cutaneous information about the human-imparted handshake are obtained by means of a sensorized glove, worn by the robot end-effector/hand.

$$\begin{cases} \dot{z}_{H,k} = \alpha_{2,k}\alpha_{4,k}; \\ z_{H,k} = \alpha_{1,k} + \alpha_{3,k}. \end{cases} \tag{7}$$

From (7), one can note that the expression for $z_{H,k}$ is the same as (5), and from (4) that $\alpha_{2,k}\alpha_{4,k} = (\dot{z}_{H,k}/\omega_k)\omega_k = \dot{z}_{H,k}$.

The information is used to synchronize the human/robot handshake, mapping the human subject kinaesthetic behaviour to the robot motion. To accomplish this, we generate a cartesian pose reference for the robot as follows:

To be consistent with the 1-DoF modelling of the human/robot handshake motion, the cartesian pose reference at time k, namely $\mathbf{u}_{P,k}$, is set as

$$\mathbf{u}_{P,k} = [\, x_0, \;\; y_0, \;\; \hat{z}_k, \;\; | \;\; \mathcal{Q}_0 \,]^T, \tag{8}$$

where x_0, y_0 are the initial linear coordinates of the end-effector along x and y, while $\mathcal{Q}_0$ is the unitary quaternion representing its initial orientation. They are required to remain constant during the handshake motion. $\hat{z}_k$ is set as

$$\hat{z}_k = \alpha_{1,k} + \alpha_{3,k} + T_{ant}\alpha_{2,k}\alpha_{4,k} = z_{H,k} + T_{ant}\dot{z}_{H,k}, \tag{9}$$

where the final term is a constant time anticipation.

The robotic arm active behaviour we wish to reproduce is obtained by setting the term T_{ant} in the definition of the control input $\hat{z}_k$. Moreover, this time anticipation allows for compensation of the intrinsic control system delay.

A schematic of the complete control/estimation procedure is shown in Fig. 5.

3.6 Arm Stiffness Control Strategies

In contrast to the handshake kinaesthetic aspect, we can obtain cutaneous information from the human side of the interaction. This is achieved with pressure sensors, placed on the robotic hand, which detect the handshake forces exerted by the human onto the robot. Here we relate this cutaneous information to both the stiffness of the manipulator and the closure of the robotic hand (see Sec. 3.2).

As shown recently (Aldrich and Skelton 2006; Baltaxe-Admony et al. 2016; Lessard et al. 2016) the human arm musculoskeletal system can be considered as a *tensegrity*

structure. Such structures are comprised of compression elements, which in the human arm are the bones, and tension elements that connect the former in suspension, like the arm muscles and fascia do. The resulting structure is flexible and compliant to external mechanical disturbances. If one wishes to obtain a certain stiffness at the endpoint of a tensegrity structure, a corresponding modulation of the stiffness across all tension elements in the structure is required. Following this, and according to the findings of Ajoudani et al. (2012), we hypothesize that there could be a coupling between the hand grasping force (i.e. end-effector stiffness) and the impedance of the arm as a whole.

In order to investigate this, we implement different control laws for the arm stiffness. In particular, the controlled stiffness of the robot K_R can be set in three different ways via its impedance control: i) to a constant maximum stiffness $K_{MAX} = 600 N/m$; ii) to a constant minimum stiffness $K_{MIN} = 100 N/m$; and iii) to a variable stiffness, related to the cutaneous human feedback via the pressure measurements, with a law similar to that presented in (11):

$$K_{VAR} = K_{MIN} + (K_{MAX} - K_{MIN})W_K \frac{\sum_{i=1}^{n} p_i}{n p_{max}}, \tag{10}$$

where W_K is a tuned constant-weight coefficient relating the cartesian stiffness value to the pressure measurements, p_i is the ith filtered pressure measurement value, n is the number of measurements and p_{max} is the pressure sensor saturation. As discussed in Sec. 3.3, the numerical values of K_{MIN} and K_{MAX} are chosen in accordance with reasonable values for the human arm cartesian impedance found in literature. These quantities are used for the linear part of the arm impedance control cartesian stiffness matrix. The angular part of the matrix is populated with the same values, damped by a constant tuned weight.

We note that the arm impedance control also allows for reducing the impact of the simplifying assumption made by modelling the handshake as a 1-DoF interaction. Indeed, during a handshake, humans also exhibit movements along different directions alongside the main motion axis. Although minor, such movements are nonetheless important for the perceived naturalness of the interaction. By employing an impedance controller for the arm, the robotic end-effector can be commanded to never behave rigidly in any linear/angular direction, even when following an 1-DoF reference trajectory.

3.7 Hand Closure Control Law

As in Vigni et al. (2019), a proportional control law is used to regulate the hand closure from the pressure sensor measurements. Specifically, the handshake control law is defined as

$$F_h = F_C + F_P = W_C h_{MAX} + W_P h_{MAX} \frac{\sum_{i=1}^{n} p_i}{n p_{max}}, \tag{11}$$

where F_h is the total force exerted by the hand, F_C is a modelled internal force and F_P is a force proportional to the human action. W_C and W_P are tuned constant-weight coefficients which relate respectively the maximum allowed hand closure h_{MAX} (set for interaction comfort purposes)

and the pressure measurements with the handshake force. Variables p_i, n and p_{max} are defined as in (10). For our robotic hand, the force F_h it exerts is proportional to its motor position, as the SoftHand employs only one actuator to activate its grasping mechanism (Catalano et al. 2014). The position of the motor is in turn related to the hand closure H, so that

$$H = K_T \theta_m = f(F_h), \tag{12}$$

where θ_m is the motor position expressed in rad/s and K_T is the conversion constant between rad/s and motor ticks. We mapped F_h to the hand closure via a function $f(\bullet)$ similar to the one from Vigni et al. (2019), as they also used a Pisa/IIT SoftHand.

3.8 Experimental Procedure

As described in Sec. 2, we defined and implemented 6 control strategies for the arm behaviour, arising from the intersection between 3 stiffness control laws ($K_R = K_{MIN}$, $K_R = K_{MAX}$, $K_R = K_{VAR}$) and 2 different kinaesthetic control laws (EKF feedback enabled $\rightarrow$ active mode, EKF feedback disabled $\rightarrow$ passive mode). The arm strategies, denoted by C_1–C_6, are summarized with their features in Table 1.

In three of them, the EKF observer trajectory feedback is sent to the robot controller, switching from the robot passive motion provided by the impedance control to an active, synchronized motion. This feedback is activated after a time of $\simeq 2s$ from the detected handshake contact by the pressure sensors, so as to ensure the convergence of the filter to the unknown sinusoidal movement imparted by the human. The detected handshake pressure measurement is also required to to exceed a prescribed threshold to activate the EKF timer.

During the experiment, the robotic arm was positioned on a fixed base so that its end-effector, i.e. the gloved hand, was in a comfortable position for performing the handshake. The control strategy for the hand closure was always set to (11). A total of 20 participants were recruited for this study (14 male, age 24–31). Participants had no reported neurological or physical injury that might affect their haptic perceptions. They were briefed about the study, and asked to sign a written consent form.

To obtain stronger results, the experiment was divided into two parts.

3.8.1 Experimental Procedure — Part 1
In the first part, a randomized sequence of the 6 handshake control strategies described in Sec. 3.6 was presented to each participant. Every control strategy appeared in the sequence three times, for a total of 18 handshakes per subject. After each handshake, the subject was asked to rate the interaction on five Likert-scale questions, which were already used in (Vigni et al. 2019). Specifically, the first two questions rate the quality and the human-likeness of the handshake itself, the subsequent two rate the responsiveness of the robotic arm and if it leads or not the interaction, and the last one rates the perceived personality of the robot. The questions, listed in Table 2, make use of a modified 7-point Likert scale as in Vigni et al. (2019).

3.8.2 Experimental Procedure — Part 2
In the second part, two sets of three consecutive handshakes were

	Question	Scale (1 to 7)
Q1	Please rate the quality of the handshake	*very poor* to *very good*
Q2	Please rate the human-likeness of the handshake	*very robot-like* to *very human-like*
Q3	Please rate the responsiveness of the robot	*not responsive at all* to *very responsive*
Q4	Who was the leader of the handshake interaction?	*I was the leader* to *the robot was the leader*
Q5	Please rate the perceived personality of the robot	*shy, hesitant, introvert* to *confident, secure, extrovert*

Table 2. Likert-Scale Proposed Questionary for the Experiment First Part

presented to the subject. In the first set the three control strategies using the EKF feedback were randomly presented, and in the second set the remaining three without the synchronization effect. The subject was asked to indicate, after each set of three, which out of the the three handshakes in the set they preferred, making this a 3-Alternative Forced-Choice (3AFC) experimental design.

3.8.3 Experimental Procedure Protocol
Each subject performed in total 24 handshakes (18 in the first part plus 6 in the second part) with the robot. The participants were told to approach the robotic hand and to choose manually a position P_0 they deemed to be comfortable to perform the handshake (the robotic arm was put in gravity compensation mode). This initial position was saved by the program and presented again to the subject for every subsequent interaction. Then the control was activated and the handshake was executed. We note that in this study each subject was instructed to perform the= handshakes in the way and with the duration they considered to be the most natural, although a maximum time limit of $30s$ was set for each handshake. Moreover, subjects were free to repeat the handshakes as many times as desired, within this time limit. In this way, we intended to simulate a realistic scenario in which every person could interact with the robot with their unique behaviour.

For each handshake, the data from the robotic arm/hand were recorded for further analysis: end-effector movements; estimated states of the observer; glove pressure sensor values; the robotic hand actuator reference; and position.

4 RESULTS

Fig. 6 shows an example of some of the *ROS* recorded data for one handshake from the first part of the experiment. The control strategy visualized here is C_5, so both the effects of the synchronization and of the stiffness modulation are visible. Fig. 6a shows the robot end-effector pose and
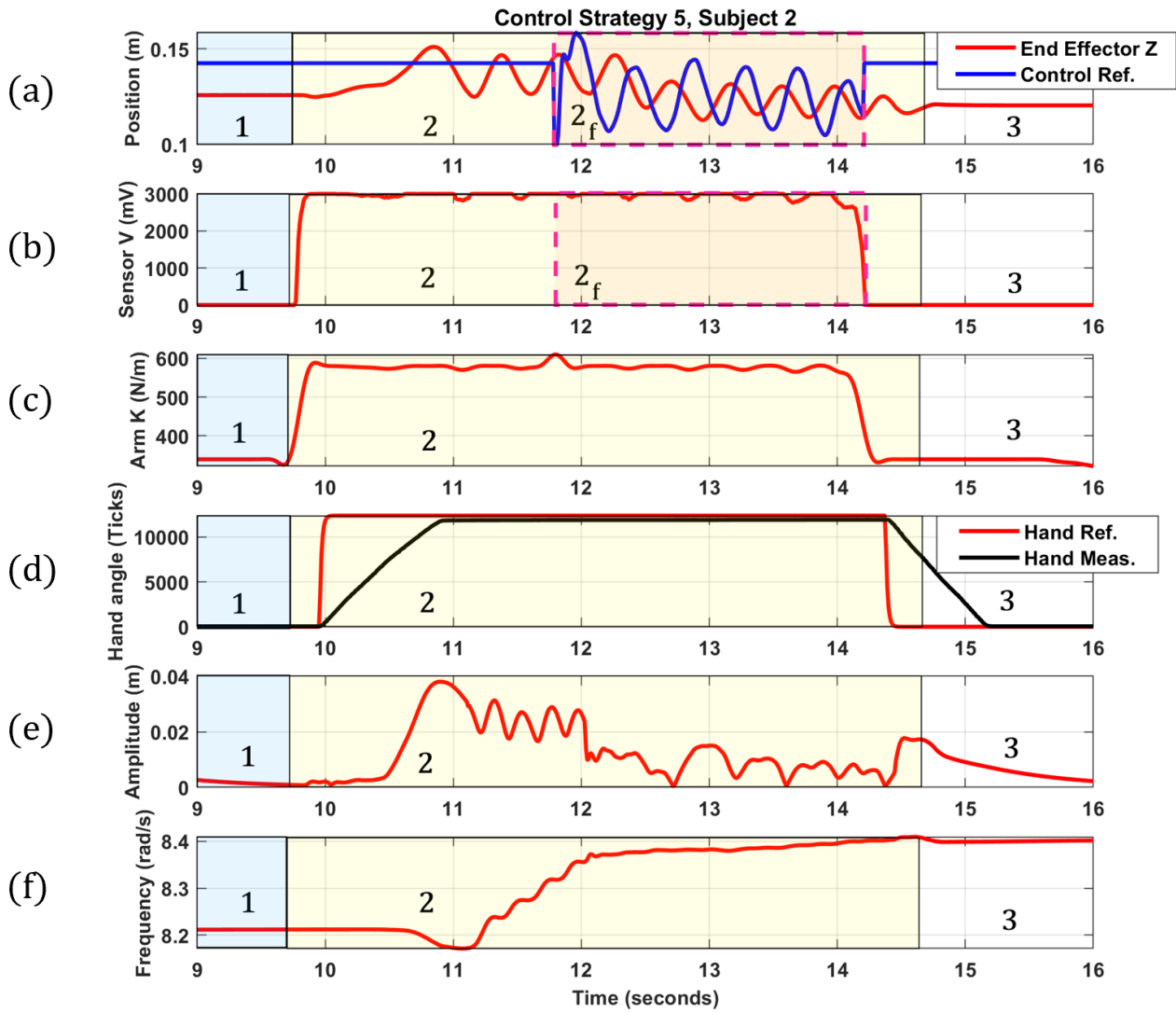
Figure 6. Sample of recorded data (7 seconds) for a handshake interaction during the experiment first part. The strategy employed here is C_5 (synchronization enabled, variable stiffness). The various phases of the human interaction with the robot are highlighted with different colors. Figure a) shows the values along the Z coordinate of the robot end-effector pose and the control input to the end-effector. Figures b) and c) show the values of the pressure measurement and of the linear stiffness of the impedance control. Figure d) focuses on the SoftHand and visualizes its reference and actual motor angles. In figures e) and f) two estimated states from the EKF (handshake amplitude and frequency) are shown.

| *p*-value Source | Quality | Response on Handshake | | | |
		Human − Likeness	Responsiveness	Leader	Personality
Synchronization	0.233	0.267	0.001	0.514	0.370
Stiffness	0.679	0.976	0.881	0.079	0.258
Subject	0	0	0	0	0
Sync./Stiffness	0.221	0.179	0.691	0.192	0.100
Sync./Subject	0.153	0.002	0	0.114	0.005
Stiffness/Subject	0.689	0.475	0.545	0.066	0.595

Table 3. N-way ANOVA Test Results. The significant p-values are highlighted in red. p-values of zero indicate $p < 10^{-4}$.

the control input to the end-effector, expressed in the end-effector frame Z-coordinate along which the handshake occurs. Figs. 6b and 6c show the pressure measurement value and the current value of the linear stiffness in the impedance control stiffness matrix. Fig. 6d visualizes the SoftHand reference and actual motor angles. Finally, Figs. 6e and 6f present two handshake motion estimated states from

the EKF, i.e. the handshake amplitude and frequency. The phase shift of the controller reference can be appreciated in Fig. 6a, where the end-effector current motion, imparted by the human, is shown in red, while the arm control reference, given by the EKF, is shown in blue.

The various phases of the human interaction with the robot are highlighted with different colors. In phase 1, the subject
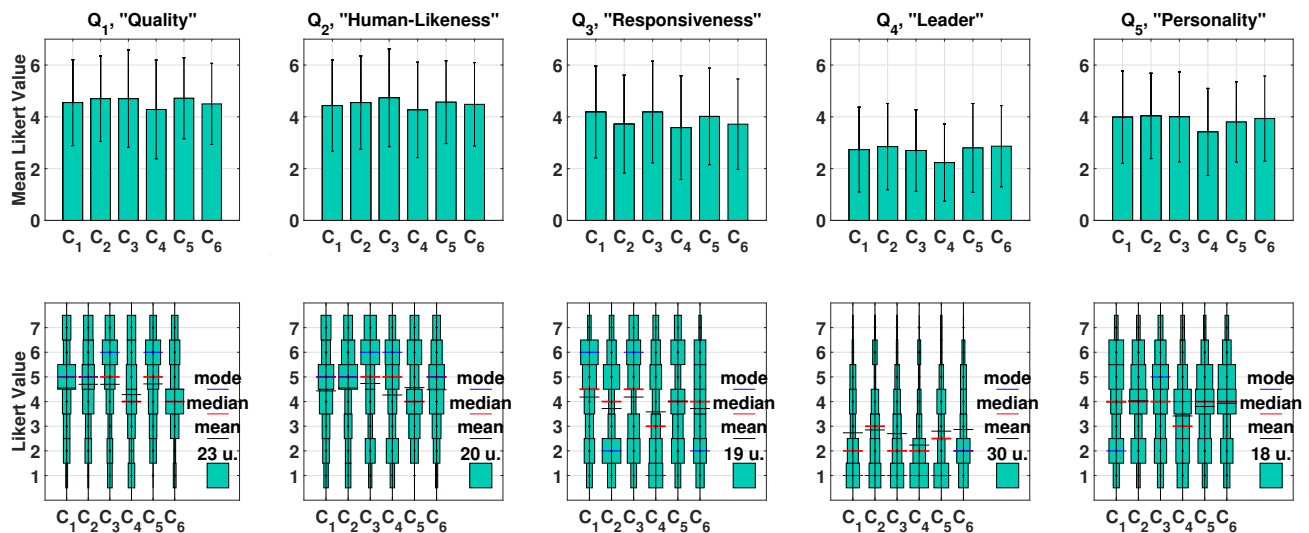
Figure 7. Statistical analysis on the totality of the Likert responses. The first row of subfigures shows the mean response of every strategy for each Likert question. Black bars show the standard deviation. The second row of subfigures presents the histograms of the response data distribution for the same question on the first row. The control strategies are labelled from C_1 to C_6 as in Tab.1. The mean, mode and median values for each strategy are shown. A unitary sample with the number of units (u.) it represent on the histogram is also shown for each subfigure.

is still approaching the robot hand. In phase 2 they makes contact with the hand, as can be seen from the pressure plot, and the hand begins to close. At the same time, the arm stiffness is increased accordingly. The subject then executes a sinusoidal handshaking motion. After $2s$ of detected contact, the EKF feedback is enabled, which is highlighted in phase 2_f. Next, an active human-robot handshake occurs for a few seconds, before being interrupted by phase 3 when the subject releases the SoftHand.

The consolidated response data distributions for every strategy and each question are shown with horizontal histograms in the second row of Fig. 7. To analyse the responses from the handshake experiments, we first computed the participant mean response for each control strategy as shown in the first row of Fig. 7.

We found that questions Q_1 and Q_2 (pertaining respectively to the quality and human-likeness) were positively rated for every strategy. For Q_1, the mean responses for each strategy (from C_1 to C_6) were respectively: 4.55, 4.70, 4.70, 4.28, 4.72 and 4.50. The same quantities for Q_2 were: 4.43, 4.55, 4.73, 4.27, 4.57 and 4.48. For Q_3 (i.e. for the responsiveness of the handshake) the mean responses were slightly lower: 4.18, 3.72, 4.18, 3.58, 4.02 and 3.72. For Q_4, pertaining to the initiative of the robot, the mean response for each strategy was respectively: 2.73, 2.85, 2.70, 2.23, 2.80 and 2.87. The same quantities for Q_5 (perceived personality of the robot) were: 3.98, 4.03, 4.00, 3.42, 3.80 and 3.93.

Given the shape of the distributions in Fig. 7 (second row), which hints a non unimodal behaviour across different subjects, we considered a $2 \times 3 \times n_S$ (n_S being the number of subjects) factor experiment design to separate the effects of the 2 strategies on arm motion and of the 3 strategies on arm stiffness from the individual subject tendencies. Specifically, we used a N-way ANOVA test, in order to study the interaction between every experiment feature. For each

question, the collected data for each subject was arranged in an ANOVA-style matrix as:

$$\text{Synchronization Enabled} \{ \begin{bmatrix} \mathcal{D}_{1,j,k} & \mathcal{D}_{3,j,k} & \mathcal{D}_{5,j,k} \\ \mathcal{D}_{2,j,k} & \mathcal{D}_{4,j,k} & \mathcal{D}_{6,j,k} \end{bmatrix}$$
$$\underbrace{\phantom{\mathcal{D}_{1,j,k}}}_{K_{MAX}} \underbrace{\phantom{\mathcal{D}_{4,j,k}}}_{K_{MIN}} \underbrace{\phantom{\mathcal{D}_{6,j,k}}}_{K_{VAR}}$$

where $\mathcal{D}_{i,j,k}$ represents the response data collected for the ith control strategy, the jth question and the kth subject.

First, we checked the three ANOVA prerequisites for the data (for each question), i.e. i) independence of cases, ii) normal distribution of the residuals, and iii) homogeneity of variances. While condition i) is satisfied by the randomization of the control strategy presentation order we defined before the experimentation, we carried specific tests to investigate ii) and iii).

Regarding condition ii), we employed the Lilliefors test to check the normality of the residual distribution. Apart from the Personality question data, the other data populations do not satisfy the hypothesis of normality, which points towards strong expectations of the subjects regarding the respective interaction aspects. However, considering the large number of data points and the high robustness of the ANOVA test in this regard (see e.g. Carifio and Perla (2007) and Glass et al. (1972)) we deem the ANOVA results valid nonetheless.

For condition iii), we used the Brown-Forsythe test to verify the homogeneity of variances. This condition is more critical w.r.t the previous one, as the Fisher test (on which ANOVA is based) is less robust to its violations (see again Carifio and Perla (2007)). In this case, the hypothesis of non-homogeneity was rejected for each question, with respective p-values of 0.3359, 0.6630, 0.9428, 0.9128 and 0.5728.

Another confirmation of the large variability of subject behaviours (which arises in part because we asked every subject to interact with the robot in the way they preferred) can be seen from Fig. 8 in terms of mean number of
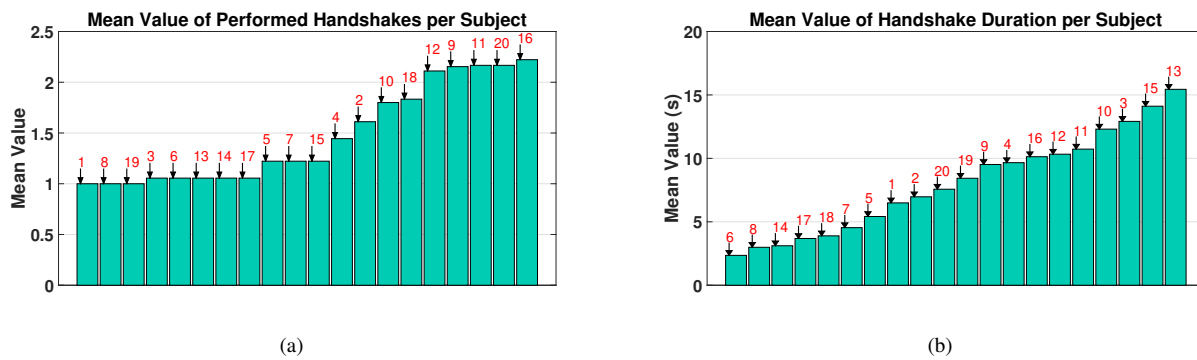
(a)

(b)

Figure 8. Figure shows, for each subject during the experimentation part 1 tasks, a) the mean value of handshake performed, and b) the mean value of the total handshake duration. The number of the subject is shown in red.

handshakes and mean duration of handshake per condition per subject (the corresponding subject number is highlighted in red). In Fig. 9, we show the mean values of the grasping pressure excerted by the human for each strategy, along with the mean of the standard deviation of the same readings.

The results for the N-way ANOVA test are summarized in Table 3, where the significant p-values are highlighted in red. p-values of zero indicate $p < 10^{-4}$. The table rows indicate the p-value source, which assesses the significance of the effect of i) the synchronization, ii) the stiffness control law, iii) the current subject, iv) the interaction between the effects of synchronization and stiffness, v) the interaction between the effect of synchronization and the current subject, and vi) the interaction between the effect of stiffness and the current subject. The table columns represent the handshake aspects considered in the Likert questions.

From the N-way ANOVA test, it can be firstly seen from the third row of Tab. 3 that the subject individuality does have a strong effect on every question, as expected from the previous discussion. The synchronization appears to be highly significant in terms of responsiveness of the robot (third column), both on its own and in interaction with the subject. A less marked effect of the synchronization feature is also present in terms of the human-likeness of the handshake (second column). We can observe that the interaction between the synchronization and the subject is also significant in terms of the robot perceived personality. Finally, no significant effects are found in terms of quality of the handshake (first column) and on the perceived leader of the interaction (fourth column), apart from the subject individuality. In general, no significant effect of the stiffness was found.

Finally, we conducted post-hoc tests using Tukey's Honestly Significant Difference Procedure. In the only significant result not related to the subjectivity effects, i.e. the feedback feature in the "Responsiveness" question, the test revealed that the responses arising from the active motion data group were closer to the upper end of the scale (corresponding to a robot perceived as more active) compared to the passive motion data group, as shown in Fig. 10a.

Regarding the Subjectivity feature and its interaction with Synchronization, the Tukey test confirmed the variability between each subject. Most subject data groups were found to have a marginal mean significantly different from

many others. An example of this can be seen for the "Responsiveness" question in Fig. 10b.

The results from the second part of the experiment are presented in Fig. 11. When directly asked to perform a choice between three handshakes, the responses follow the same trend as for the strategies with and without use of the observer, although the differences are more pronounced in the first case. The majority of the subjects choose the strategies employing a low, constant stiffness (i.e. the 45% for both C_3 and C_4) while the variable stiffness was the least chosen (respectively by the 20% for C_5 and the 25% for C_6).

5 DISCUSSION

The results presented in the previous Section show that the use of synchronization and also the arm stiffness regulation does have effect on the human-robot handshake. These results were obtained under relatively unconstrained conditions, where participants were free to interact with the robot as they preferred: participants were instructed to perform a handshake in the way and with the duration they considered to be the most natural and appropriate. Moreover, each subject was free to repeat the handshakes as many times as desired, within a time limit. This is echoed by the strong significance of the subject individuality for each Likert question response, and shown in Figs. 8. Additional evidence of such behaviour is shown in Fig. 9, which allow us to see how every subject applies approximately the same signature grasp force across all strategies. The high variability in the grasp forces is confirmed by the pressure sensing (mean) standard deviation, although this could also have arisen from the periodic oscillations of the handshaking motion.

Regarding the other features of the experiment, the effect of the feedback seems to dominate the effect of stiffness. Although no significant values are found for the effect of the stiffness in experiment 1, experiment 2 shows stiffness to also have an impact. The lack of significant effects of the impedance strategies on the perceived personality and initiative of the robot would seem to be consistent with (and complementary to) the results from the same questions in Vigni et al. (2019), as i) the subjects considered this aspect to only pertain to the closure of the hand rather than also the arm movement, and ii) the hand closure feedback law was indeed always the same.
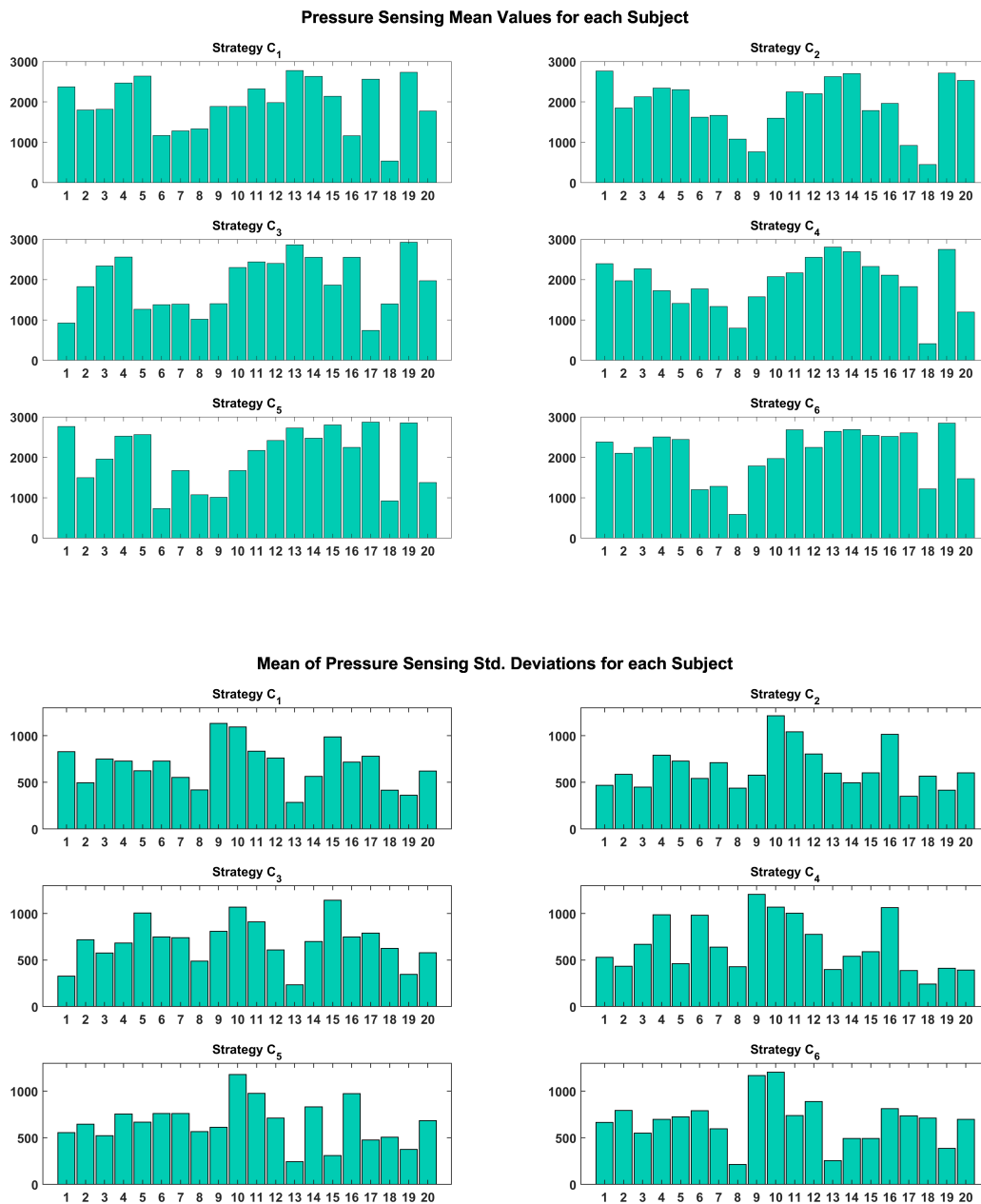
Figure 9. Figure shows, for each subject and each strategy during the experiment part 1 tasks, the mean value of the pressure sensing they activate during the handshakes, along with the mean of the standard deviation on the same readings. The control strategies are labelled from C_1 to C_6 as in Tab.1.

In our study, the traits addressed in Q_1 and Q_2 have been, in general, positively rated by the participants: from Fig.7 it can be seen that for this questions the mean values are almost always above the Likert scale median value. Thus, the hand closure was in general perceived as comfortable, of good quality and acceptably human-like. This is in contrast with a previous handshaking study with the SoftHand (Knoop et al. 2017) where its performed handshake was perceived as uncomfortable. The improvement in performance can be attributed to the use of the soft silicon glove, based on the motivations on its design reported in Section 3.2. An additional factor could be the incorporation of the control law proposed by Vigni et al. (2019).

Regarding the silicone glove itself, informal post-experiment interviews indicated that, in general, the gloved hand is not perceived as uncomfortably bulky to grasp, even if looks less ergonomic compared to the bare hand. Moreover, the glove is highly compliant as it is made from a soft silicone. Also, the subjects liked the sensation of the gloved hand envelope. Still, an interesting direction for future work would be to optimize the glove design regarding the quantity of used silicone, as in this first work we prioritized the mechanical protection of the embedded sensors.

For question Q_3, about responsiveness, it can be noted that the mean responses for the strategies employing the EKF feedback to simulate an active behaviour of the robot
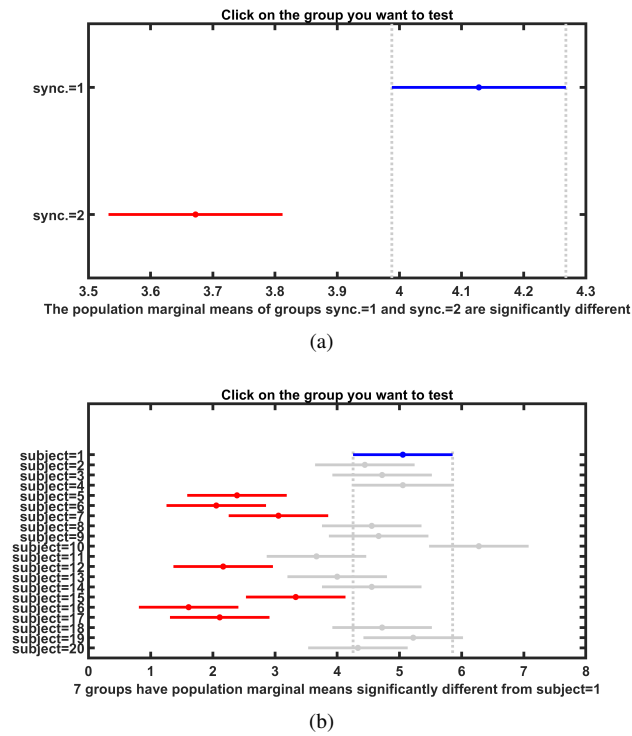
(a)

(b)

Figure 10. Figure shows an example of the carried post-hoc testing results, for a) the feedback feature and b) the subjectivity feature. Both features refer to the "Responsiveness" question. In a), "sync. = 1" refers to the active motion data group, and "sync. = 2" to the passive motion data group.
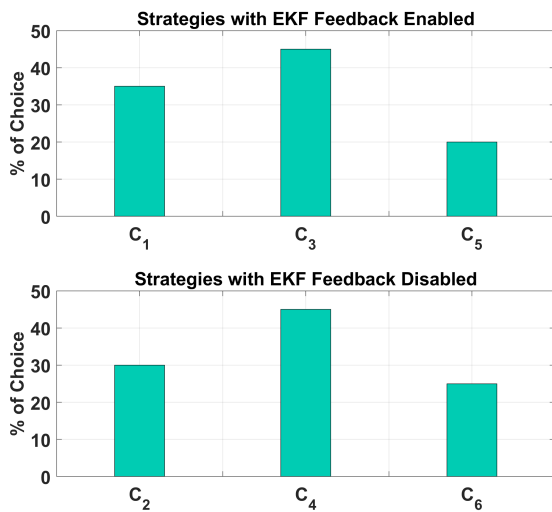

Figure 11. Results of forced-choice three-way comparisons from experiment part 2. The control strategies are labelled from C_1 to C_6 as in Tab.1.

are higher than the same quantities for the strategies which do not use it. The responsiveness and, in a minor way, the human-likeness of the handshake and the perceived personality of the robot appear to be related to the effect of the motion feedback. The responsiveness, in particular, is shown to be directly and intuitively related to the active/passive behaviour of the robotic arm.

For question Q_4, regarding the leadership of the interaction, responses are towards the lower end of the Likert scale, so participants felt that they were the leaders during the handshake. This could be explained by considering that the human was always in charge of the handshake initiation (via making contact with the robot hand), while the robot was static in the initial position P_0, which would likely have contributed to the perception of the interaction leader. This perception could be changed e.g. by performing an approach motion of the arm before requesting the handshake from the subject, as in Jindai et al. (2015). We also hypothesize that the term T_{ant} plays a role on both the "leadership" and the "responsiveness" aspects of the handshake. Thus, in future works it would be interesting to investigate the direct relationship between different values of T_{ant} and the perception of the subject. Finally, enabling visual and/or auditory stimuli from the system in the experiment would likely help to simulate the intention of the robot to lead the interaction. This would be consistent with the studies reported further on in this Section.

A significant difference is observed in question Q_3, related to the synchronization effect. This latter point is in contrast with the responses of the same questions in Vigni et al. (2019), so it appears that this trait is more related to the movement of the arm rather than to the way the hand closes.

Comparing the results from experiments 1 and 2, it can be observed that the results reveal different aspects of how the experiments were perceived: in experiment 2 we asked for the overall quality to be rated, whereas in experiment 1 the questions targeted more specific qualities. Thus, while experiment 2 provides a clearer indication of which strategy should be selected for optimum performance, the forced-choice ratings give no indications about the reasoning behind the preferred ratings. Moreover, as experiment 2 placed the active and passive strategies in separate blocks, one would naturally expect that participants would make clearer distinctions between the different stiffness conditions within each block, compared to experiment 1.

It is interesting to note that, as shown by the results from the second part of the experiment, the participants seem to prefer a low, constant stiffness when forced to choose between different handshakes, both with an active or passive robot behaviour. It would therefore appear from these aggregated results that, in general, participants would prefer to interact with a robot that is perceived as less dominant. This effect is not visible in the results from the first phase of the experiment, which could be explained by the caution that most people may approach a full robotic arm handshake with, and by the consequent desire to be in control of the interaction. This is also consistent with a study conducted in Tsalamlal et al. (2015), where it was shown that the use of haptic stimuli in a human-robot handshake maps mostly to the *Dominance* and *Arousal* emotional dimensions. It would be interesting to investigate the same experiment while adding also visual/facial stimuli, as they appear to dampen the haptic *Dominance* valence. In general, subjects will focus on different aspects of a handshake when asked different kinds of questions and under different experimental designs, as indicated by experiments 1 and 2 here. It is noteworthy that the control of the arm stiffness results in a change of the perceived initiative of the robot which is more pronounced than the other traits. Although our results in experiment 1 are not significant, experiment 2 shows
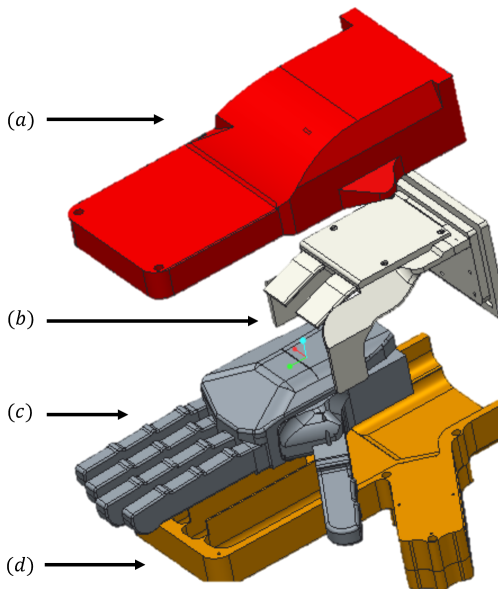
Figure 12. The main parts of the glove mould: a) back outer mould, b) circuitry core mould, c) hand core mould, d) palm-thumb outer mould.

stronger trends. We believe this to be an interesting result that warrants further study, also considering the responses to the same questions given in Vigni et al. (2019). It is worth noting that the perceived attitude/personality of a social robot is one of the most important features in its acceptance and in establishing an emotional bond with humans (Bhattacharjee and Niemeyer 2015); see, for example, the recent study in Avelino et al. (2018a), where the human willingness to help a robot whether it first introduces itself with or without a handshake has been evaluated.

Building on these last considerations and on the overall results obtained in this study, we argue that the developed system represents a step forward w.r.t. the pHRI state of the art, and could also have interesting applications in the field of social robotics. The framework presented here would appear well-suited for investigating the human perception of different robot behaviours, specifically pertaining to how robots can mimic or exhibit social interaction skills and communicate their emotions.

6 CONCLUSIONS

In this paper we have investigated the perceived naturalness of motion and personality traits associated to a soft human-robot handshake.

The investigations have been implemented on a full lightweight anthropomorphic arm, mounting a Pisa/IIT Softhand wearing a sensorized silicone glove as end-effector. The use of the custom-made silicone glove resulted in improved comfort and human-likeness of the robotic handshake compared to a previous handshaking study using the SoftHand. Several human-robot handshake experiments were performed by 20 participants, who rated the quality of the perceived interaction using Likert scales.

Our results show that the different controllers exhibit variations in the perceived personality qualities of the robot i.e. introvert/extrovert, and on its responsiveness. In

particular, the responsiveness, the human-likeness of the handshake and the perceived personality of the robot would seem to be more related to the way the arm moves rather than how the robotic hand closes. In a second experiment, the arm stiffness was found to have an effect on the overall handshaking quality, with clear trends in the preferred stiffness. The strong dependency of the results on the subjectivity of the participants is to be expected given the unconstrained nature of the experiments. Studies 1 and 2, taken together, highlight the importance of using different experimental designs for isolating and evaluating different effects. The system developed here would lend itself to multiple such studies in the field of pHRI, and also in social robotics.

Another interesting future research direction would be to perform the same experimentation employing different soft robotic hands, in order to investigate how their design influences the overall experience.

A Silicone Glove Fabrication

We choose *Ecoflex 00-30*[†] for the silicone glove, as it is soft and durable, and easy to use.

The silicone glove body is fabricated in a moulding process. Inner (*c*) and outer (*a-d*) moulds were designed to mimic the form factor of the Pisa/IIT SoftHand, along with several additional components to allow for the placement of those electronic parts inside the glove (*b*) that are not to be dipped in the silicone. The complete mould is composed of multiple 3D printed parts that can be disassembled by screws, to facilitate the extraction process while still obtaining a single part glove. The complete computer-aided design of the mould parts is shown in Fig. 12.

The glove fabrication process is shown in Fig. 13. In particular, in Fig. 13a some components of the disassembled inner mould are shown. An *o-ring* can also be seen, which is used to obtain a watertight chamber for the electronic board inside the glove, in the dorsal hand zone. In Fig. 13b we show how additional electronics components are arranged in the assembled inner mould before the main cast. These

---

[†]https://www.smooth-on.com/products/ecoflex-00-30/

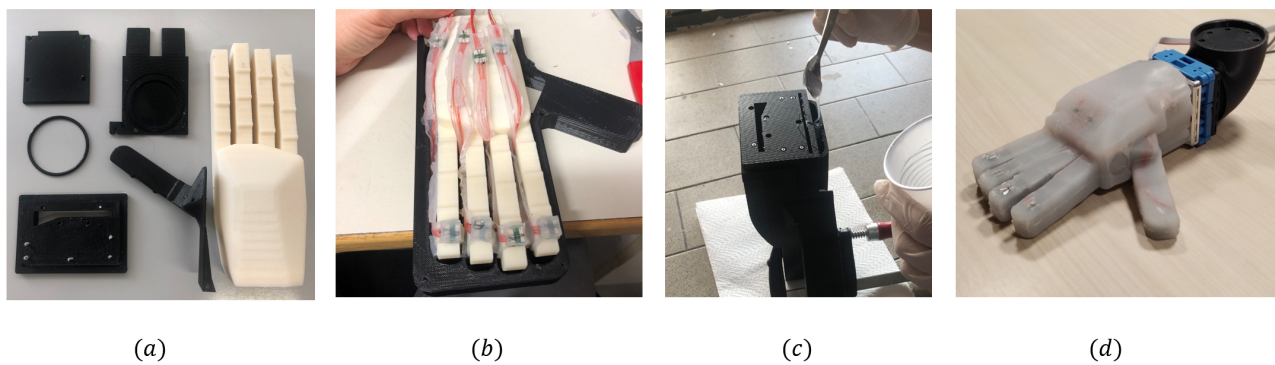| (a) | (b) | (c) | (d) |

Figure 13. Glove fabrication process. a) Inner mould disassembled components. b) Placement of electronics integrated with the silicone. c) Pouring of the silicone inside the complete mould. d) Extracted glove ready to be connected to the manipulator.

sensors (Inertial Measurements Units, IMUs) are not used in this study, but they could be employed in other experiments (e.g. similar to those presented in Bianchi et al. (2018)). Their connectors reach the watertight chamber for the electronic board. They are shown here to highlight that the silicone glove can be readily equipped with various, maybe complementary, sensors for multiple tasks, by directly casting them in the silicone. We decided here to not do this with the FSR sensors and to place them in channels directly obtained in the circuitry inner mould, as the silicone could infiltrate the gaps between their resistive layers and alter performance.

After the arrangement of the inner electronics, the complete mould is assembled. Then, silicone is poured in the mould placed in a vertical configuration (Fig. 13c). After the prescribed time for polymerization, the back outer mould is removed first. The components of the inner mould parts are then carefully unscrewed and removed, to facilitate the extraction process and to avoid damage to the integrate electronics. Once the glove has been extracted, the FSR sensor arrays are placed manually inside the obtained channels to reach the locations highlighted in Fig. 3, with their analogue circuit connected to the electronic board. A complete glove, worn by the SoftHand connected to a flange (which is the interface with the manipulator end-effector) is shown in Fig. 13d.

References

Ajoudani A, Tsagarakis NG and Bicchi A (2012) Tele-impedance: Towards transferring human impedance regulation skills to robots. In: *2012 IEEE International Conference on Robotics and Automation*. IEEE, pp. 382–388.

Aldrich J and Skelton R (2006) Backlash-free motion control of robotic manipulators driven by tensegrity motor networks. In: *Proceedings of the 45th IEEE Conference on Decision and Control*. IEEE, pp. 2300–2306.

Arns M, Laliberté T and Gosselin C (2017) Design, control and experimental validation of a haptic robotic hand performing human-robot handshake with human-like agility. In: *2017 IEEE/RSJ International Conference on Intelligent Robots and Systems (IROS)*. IEEE, pp. 4626–4633.

Artemiadis PK, Katsiaris PT, Liarokapis MV and Kyriakopoulos KJ (2010) Human arm impedance: Characterization and modeling

in 3d space. In: *2010 IEEE/RSJ International Conference on Intelligent Robots and Systems*. IEEE, pp. 3103–3108.

Avelino J, Moreno P, Bernardino A, Correia F, Paiva A, Catarino J and Ribeiro P (2018a) The power of a hand-shake in human-robot interactions. In: *2018 IEEE/RSJ International Conference on Intelligent Robots and Systems (IROS)*. IEEE, pp. 1864–1869.

Avelino J, Paulino T, Cardoso C, Nunes R, Moreno P and Bernardino A (2018b) Towards natural handshakes for social robots: human-aware hand grasps using tactile sensors. *Paladyn, Journal of Behavioral Robotics* 9(1): 221–234.

Avraham G, Nisky I, Fernandes HL, Acuna DE, Kording KP, Loeb GE and Karniel A (2012) Toward perceiving robots as humans: Three handshake models face the turing-like handshake test. *IEEE Transactions on Haptics* 5(3): 196–207.

Baltaxe-Admony LB, Robbins AS, Jung EA, Lessard S, Teodorescu M, SunSpiral V and Agogino A (2016) Simulating the human shoulder through active tensegrity structures. In: *ASME 2016 International Design Engineering Technical Conferences and Computers and Information in Engineering Conference*. American Society of Mechanical Engineers, pp. V006T09A027–V006T09A027.

Bhattacharjee T and Niemeyer G (2015) Antagonistic muscle based robot control for physical interactions. In: *2015 IEEE International Conference on Robotics and Automation (ICRA)*. IEEE, pp. 298–303.

Bianchi M, Averta G, Battaglia E, Rosales C, Bonilla M, Tondo A, Poggiani M, Santaera G, Ciotti S, Catalano MG et al. (2018) Touch-based grasp primitives for soft hands: Applications to human-to-robot handover tasks and beyond. In: *2018 IEEE International Conference on Robotics and Automation (ICRA)*. IEEE, pp. 7794–7801.

Carifio J and Perla RJ (2007) Ten common misunderstandings, misconceptions, persistent myths and urban legends about likert scales and likert response formats and their antidotes. *Journal of Social Sciences* 3(3): 106–116.

Catalano MG, Grioli G, Farnioli E, Serio A, Piazza C and Bicchi A (2014) Adaptive synergies for the design and control of the pisa/iit softhand. *The International Journal of Robotics Research* 33(5): 768–782.

Della Santina C, Piazza C, Gasparri GM, Bonilla M, Catalano MG, Grioli G, Garabini M and Bicchi A (2017) The quest for natural machine motion: An open platform to fast-prototyping articulated soft robots. *IEEE Robotics & Automation Magazine*

24(1): 48–56.

Dolan JM, Friedman MB and Nagurka ML (1993) Dynamic and loaded impedance components in the maintenance of human arm posture. *IEEE Transactions on Systems, Man, and Cybernetics* 23(3): 698–709.

Dolcos S, Sung K, Argo JJ, Flor-Henry S and Dolcos F (2012) The power of a handshake: neural correlates of evaluative judgments in observed social interactions. *Journal of Cognitive Neuroscience* 24(12): 2292–2305.

Giannopoulos E, Wang Z, Peer A, Buss M and Slater M (2011) Comparison of people's responses to real and virtual handshakes within a virtual environment. *Brain research bulletin* 85(5): 276–282.

Glass GV, Peckham PD and Sanders JR (1972) Consequences of failure to meet assumptions underlying the fixed effects analyses of variance and covariance. *Review of educational research* 42(3): 237–288.

Jindai M, Ota S, Ikemoto Y and Sasaki T (2015) Handshake request motion model with an approaching human for a handshake robot system. In: *2015 IEEE 7th International Conference on Cybernetics and Intelligent Systems (CIS) and IEEE Conference on Robotics, Automation and Mechatronics (RAM)*. IEEE, pp. 265–270.

Knoop E, Bächer M, Wall V, Deimel R, Brock O and Beardsley P (2017) Handshakiness: Benchmarking for human-robot hand interactions. In: *2017 IEEE/RSJ International Conference on Intelligent Robots and Systems (IROS)*. IEEE, pp. 4982–4989.

Lessard S, Castro D, Asper W, Chopra SD, Baltaxe-Admony LB, Teodorescu M, SunSpiral V and Agogino A (2016) A bio-inspired tensegrity manipulator with multi-dof, structurally compliant joints. In: *2016 IEEE/RSJ International Conference on Intelligent Robots and Systems (IROS)*. IEEE, pp. 5515–5520.

Orefice PH, Ammi M, Hafez M and Tapus A (2018) Pressure variation study in human-human and human-robot handshakes: Impact of the mood. In: *2018 27th IEEE International Symposium on Robot and Human Interactive Communication (RO-MAN)*. IEEE, pp. 247–254.

Papageorgiou D and Doulgeri Z (2015) A kinematic controller for human-robot handshaking using internal motion adaptation. In: *2015 IEEE International Conference on Robotics and Automation (ICRA)*. IEEE, pp. 5622–5627.

Siciliano B, Sciavicco L, Villani L and Oriolo G (2010) *Robotics: modelling, planning and control*. Springer Science & Business Media.

Tsalamlal MY, Martin JC, Ammi M, Tapus A and Amorim MA (2015) Affective handshake with a humanoid robot: How do participants perceive and combine its facial and haptic expressions? In: *2015 International Conference on Affective Computing and Intelligent Interaction (ACII)*. IEEE, pp. 334–340.

Tsuji T, Morasso PG, Goto K and Ito K (1995) Human hand impedance characteristics during maintained posture. *Biological cybernetics* 72(6): 475–485.

Vigni F, Knoop E, Prattichizzo D and Malvezzi M (2019) The role of closed-loop hand control in handshaking interactions. *IEEE Robotics and Automation Letters* 4(2): 878–885.

Wang Z, Peer A and Buss M (2009) An hmm approach to realistic haptic human-robot interaction. In: *World Haptics 2009-Third Joint EuroHaptics conference and Symposium on Haptic Interfaces for Virtual Environment and Teleoperator Systems*. IEEE, pp. 374–379.